

Supporting Information

A Phosphoramidite-Based [FeFe]H₂ase Model Complex Displaying Fast Electrocatalytic Proton Reduction

Sofia Derossi,^a René Becker,^a Ping Li,^a František Hartl^{*a,b} and Joost N.H. Reek^{*a}

a) Van 't Hoff Institute for Molecular Sciences, University of Amsterdam, Science Park 904, 1098 XH, Amsterdam, The Netherlands. Fax: (+31) 205255604; Tel: (+31)205255265; E-mail: j.n.h.reek@uva.nl

b) Department of Chemistry, University of Reading, Whiteknights, Reading RG6 6AD, United Kingdom. Fax: (+44)1183786331; Tel: (+44)1183786795; E-mail: f.hartl@reading.ac.uk

Methods	2
Syntheses	3
UV-vis and fluorescence spectroscopy	5
NMR spectroscopy	8
Electrochemistry	9
Infrared spectroscopy	14
Spectroelectrochemistry	15
References	16

Methods

General procedures. All syntheses were carried out under an argon atmosphere, using standard Schlenk techniques. For all purifications involving column chromatography, a column with dry silica was prepared beforehand and left under vacuum overnight; the chromatography was performed under inert atmosphere with degassed solvents. All ^1H and ^{31}P NMR spectra were recorded on a Bruker AV 400 MHz spectrometer. IR spectra were recorded on a Bruker Vertex 70v FTIR spectrometer.

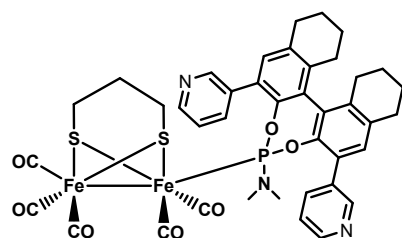
Spectroelectrochemistry. IR spectroelectrochemical measurements were performed with an optically transparent thin-layer electrochemical (OTTLE) cell¹ equipped with CaF_2 optical windows and a minigrad platinum working electrode (32 wires per cm). The optical beam can pass directly through the working electrode, allowing the redox processes taking place in the thin solution layer surrounding the working electrode to be monitored spectroscopically. The controlled-potential electrochemical conversions were carried out with a PA4 potentiostat (EKOM, Polná, Czech Republic). A slow scan rate of 2 mV/s was applied to allow quantitative electrochemical conversion. The spectra were recorded at different potential values on the thin-layer voltammograms; the the potential sweep was paused during the recording. The solutions were prepared in a similar fashion described for the other electrochemistry experiments. IR spectra were recorded on a Bruker Vertex 70v FTIR spectrometer.

Electrochemistry. Cyclic voltammetry was performed on 1 mM solutions of the Fe_2 complexes in butyronitrile containing 0.1 M $n\text{Bu}_4\text{NPF}_6$ as the supporting electrolyte. The voltammograms were recorded using a Metrohm 663 VA stand in conjunction with a PGSTAT302N potentiostat, a static mercury drop electrode (SMDE; drop size 2) as a working electrode, a glassy carbon rod as an auxiliary electrode and a double-junction reference electrode (inner compartment: 3 M $\text{KCl}_{(\text{aq})}/\text{Ag}$; outer compartment: 0.1 M $n\text{Bu}_4\text{NPF}_6$ in butyronitrile). Before every measurement, the solution was purged with nitrogen for 1 minute. Single equivalents of acetic acid were added as a 10% v/v solution in butyronitrile. To convert the potential values of the 3 M KCl/Ag reference to Fc/Fc^+ , a correction factor of -0.43 V was used.

Steady state absorption and emission. UV-vis measurements were conducted on a Cary spectrophotometer and a Scinco S3100 diode array spectrophotometer. Luminescence measurements were recorded using a Spex Fluorolog 3 spectrofluorimeter. A typical UV-vis and luminescence titration experiment was performed using two stock solutions. The solution of the chromophore (host) was normally $\sim 8 \cdot 10^{-5}$ M of ZnTPP in DCM. The solution of the diiron catalyst (guest) was about 20 times more concentrated, and was prepared by dissolving the complex in the host solution (in order to keep the concentration of the chromophore constant throughout the experiment). For the UV-vis titration, a 1 mm quartz cuvette was employed, containing 200 μL of host solution alone at the starting point. In the case of the luminescence titration, a 1 cm quartz cuvette was filled with 2 mL of the host solution alone at the starting point. In both cases, known aliquots of the guest solution were added to the cuvette, followed by recording of a spectrum. The excitation wavelength in case of the luminescence experiment was chosen to match the isosbestic point found in the UV-vis titration.

Materials. Unless stated otherwise, all chemicals were commercially available and employed without further purification. All solvents were purified *via* SPS (Solvent Purification System) or *via* distillation and degassed by mean of argon bubbling prior to use. The phosphoramidite linkers *mPyPA* and *PhPA*,² the hexacarbonyl complex $[\text{Fe}_2(\mu\text{-pdt})(\text{CO})_6]$,³ and the diiron catalysts **1**⁴ and **3**⁵ were prepared according to the previously published methods.

Syntheses



$[\text{Fe}_2(\mu\text{-pdt})(\text{CO})_5(\textit{mPyPA})]$ (**2**) MeCN (10 mL) was added to a Schlenk vessel, charged with $[\text{Fe}_2(\mu\text{-pdt})(\text{CO})_6]$ (165 mg, 0.428 mmol), *mPyPA* (223 mg, 0.428 mmol) and dry Me_3NO (53 mg, 0.48 mmol). The red solution was stirred and full conversion was achieved in 1 h, as monitored by IR spectroscopy. The solvent was removed under vacuum, and the resulting red-brown solid was purified on a silica gel column, using 3% MeOH in DCM as the eluent. The product was collected as an intense red band. Yield: 60%.

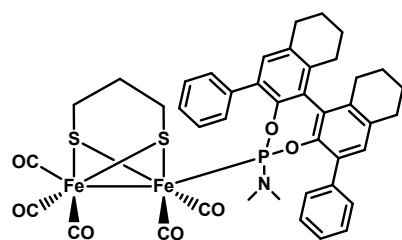
IR: $\nu(\text{CO})/\text{cm}^{-1}$ in MeCN 2047(s), 1993(s), 1975(s) and 1962(m).

¹H NMR: aromatic region in CDCl_3 δ 8.91 (dd, 2H), 8.59 (dd, 1H), 8.45 (dd, 1H), 8.21 (dt, 1H), 8.02 (dt, 1H), 7.34 (m, 2H), 7.30 (s, 1H) and 7.24 (s, 1H) ppm.

³¹P NMR: in CDCl_3 δ 187.5 ppm.

MS (FAB⁺) for $\text{C}_{40}\text{H}_{38}\text{Fe}_2\text{N}_3\text{O}_7\text{PS}_2$: m/z calculated 879.06, observed 880.07 $[\text{M} + \text{H}^+]$.

UV-vis spectrum: in DCM 349 nm ($\epsilon = 12320 \text{ cm}^{-1}\text{M}^{-1}$), shoulder at 491 nm ($\epsilon = 1230 \text{ cm}^{-1}\text{M}^{-1}$). The residual absorption at 600 nm has a molar absorption coefficient of $90 \text{ cm}^{-1}\text{M}^{-1}$.



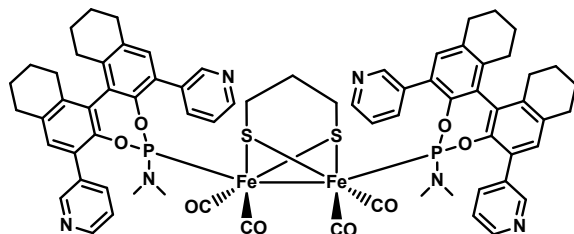
$[\text{Fe}_2(\mu\text{-pdt})(\text{CO})_5(\text{PhPA})]$ (**4**) MeCN (10 mL) was added to a Schlenk vessel, charged with $[\text{Fe}_2(\mu\text{-pdt})(\text{CO})_6]$ (202 mg, 0.523 mmol), *PhPA* (300 mg, 0.577 mmol) and Me_3NO (64 mg, 0.57 mmol). The red solution was stirred and abundant precipitate formed within one hour. The reaction was monitored by IR spectroscopy. The solvent was removed under vacuum, and the crude solid was purified on a silica gel column, using pure DCM as the eluent. The desired product eluted in the first fraction and was isolated as a bright red solid. Yield: 62%.

IR: $\nu(\text{CO})/\text{cm}^{-1}$ in MeCN 2045(s), 1992(s), 1973(m) and 1961(sh).

^1H NMR: aromatic region in CD_2Cl_2 δ 7.82(dd, 2H), 7.77 (dd, 2H), 7.47 (td, 2H), 7.38-7.31 (m, 5H) and 7.24 (tt, 1H) ppm.

^{31}P NMR: in CD_2Cl_2 δ 186.1 ppm.

MS (FAB $^+$): for $\text{C}_{42}\text{H}_{40}\text{Fe}_2\text{NO}_7\text{PS}_2$, m/z calculated 877.07, observed 878.09 [$\text{M} + \text{H}^+$].



[Fe $_2$ (μ -pdt)(CO) $_4$ (*m*PyPA) $_2$] (5) The disubstituted complex **5**, was synthesized as a disproportionation product of **2**. A Schlenk vessel was charged with **2** (108 mg, 123 μmol) and dexamethylcobaltocene, CoCp_2^* . The solids were dissolved in THF (8 mL) and the resulting solution was stirred for 2 h. The solvent was removed under vacuum and the product was purified by chromatography on a silica column, using 4% MeOH in DCM as the eluent. The product eluted as the last, third band. Yield: 22%.

IR: $\nu(\text{CO})/\text{cm}^{-1}$ in MeCN 2011(s), 1965(s), 1948(s).

^1H NMR: aromatic region in CDCl_3 δ 8.89 (dd, 1H), 8.82 (m, 3H), 8.63 (dd, 1H), 8.53 (dd, 1H), 8.29 (dd, 1H), 8.18 (dd, 1H), 7.97 (m, 3H), 8.01 (td, 2H), 7.32 (m, 4H), 7.14 (m, 2H) and 7.10 (m, 2H) ppm.

^{31}P NMR: in CDCl_3 δ 187.5 ppm.

MS (FAB $^+$) for $\text{C}_{71}\text{H}_{70}\text{Fe}_2\text{N}_6\text{O}_8\text{P}_2\text{S}_2$: m/z calculated 1372.29, observed 1373.30 [$\text{M} + \text{H}^+$].

UV-vis and fluorescence spectroscopy

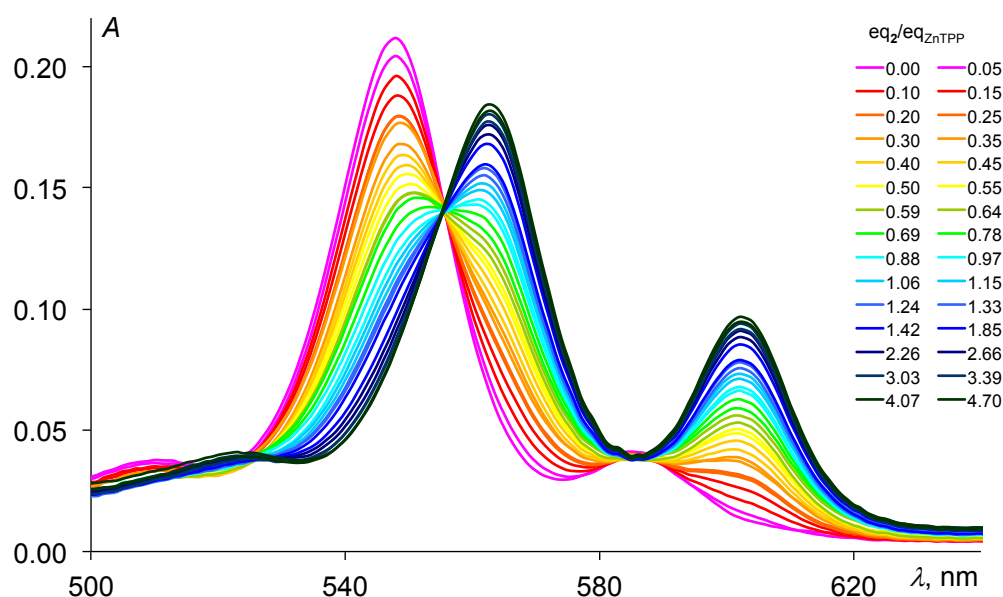


Figure S1 UV-vis spectra showing the titration of ZnTPP with **2** in DCM. Only the Q-bands of the porphyrins are shown. The first point of the titration corresponds to pure ZnTPP ($8.8 \cdot 10^{-5}$ M, pink curve); the last point corresponds to total addition of 4.7 equivalents **2** (dark blue line). The formation of the assembly is accompanied by a marked red shift of the absorption bands.

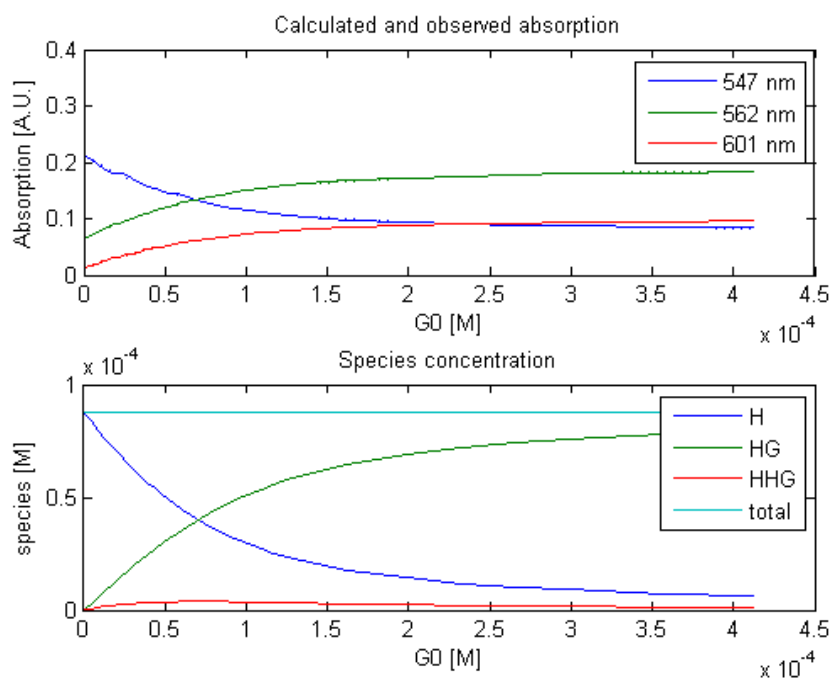


Figure S2 Association constant fitting using Matlab for the titration in Fig. S1.

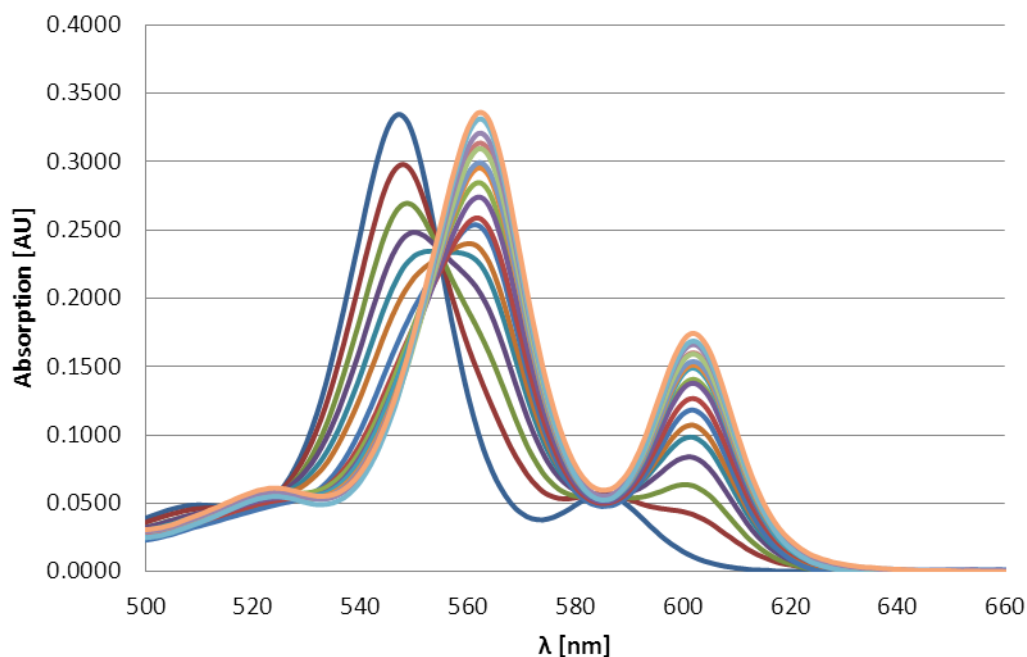


Figure S3 UV-vis spectra showing the titration of ZnTPP with *m*PyPA in DCM. Only the Q-bands of the porphyrins are shown. The first point of the titration corresponds to pure ZnTPP ($8.0 \cdot 10^{-5}$ M, blue curve); the last point corresponds to a total addition of 21 equivs *m*PyPA (orange line). The formation of the assembly is accompanied by marked red shift of the absorption bands.

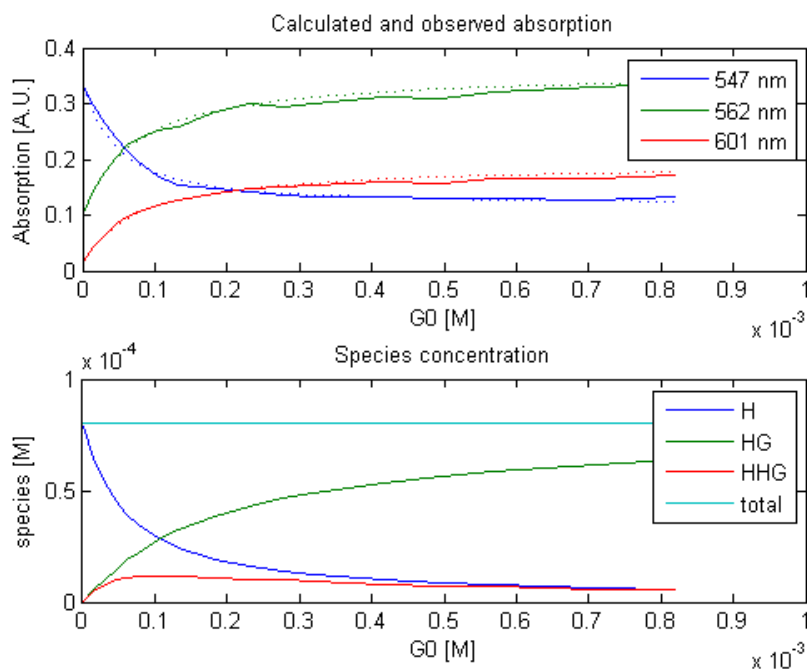


Figure S4 Association constant fitting using Matlab for the titration in Fig. S3.

Determination of association constants

Association constants were calculated by curve fitting on three wavelengths (547, 562 and 601 nm) with different constraints:

1. Two association constants per wavelength.
2. Two overall association constants, fitted on all wavelengths simultaneously.
3. One overall association constant, fitted on all wavelengths simultaneously.

For the titration data shown in Figs S1 and S3, only the last constraint yielded values for the association constants (K_{a1} and K_{a2}) and absorptivities ($\epsilon_{HG,547nm}$, $\epsilon_{HG,562nm}$, $\epsilon_{HG,601nm}$, $\epsilon_{HHG,547nm}$, $\epsilon_{HHG,562nm}$, $\epsilon_{HHG,601nm}$) that matched the expected values, namely K in the order of 10^3 - 10^4 M^{-1} , and $\epsilon_{HHG} \approx 2 \cdot \epsilon_{HG}$ for 562 and 601 nm.

Model:

$$2 \cdot K_{a1} = [HG]/([H] \cdot [G])$$

$$0.5 \cdot K_{a2} = [HHG]/([HG] \cdot [H])$$

The implemented procedure is as follows (H is host (ZnTPP) and G is guest):

- Make initial guesses for K and ϵ
- Minimize the following routine using `fminsearch` and initial guesses:
 - Calculate [H], [HG] and [HHG] iteratively:
 1. Calculate [HG] from [HHG] using:
$$u = [H]_0 - 2 \cdot [HHG] \quad v = [G]_0 - [HHG]$$
$$[HG] = \frac{2 \cdot K(u + v) + 1 - \sqrt{(2 \cdot K(u + v) + 1)^2 - 16 \cdot uvK^2}}{4 \cdot K}$$
 2. Calculate [HHG] from [HG] using:
$$[HHG] = \frac{0.5 \cdot K[HG]([H]_0 - [HG])}{1 + K[HG]}$$
 3. Calculate [H] from [HG] and [HHG] using:
$$[HG] = [H]_0 - [HG] - 2 \cdot [HHG]$$
 4. If the three concentrations have not converged to constant values, go back to 1.
 - Calculate the expected absorption using K , ϵ , [H], [HG] and [HHG]
 - Calculate compound error (expected absorption – observed absorption) for all three wavelengths
- Minimization returns new values for K and ϵ
- If minimization has converged, return K and ϵ . Otherwise, minimize again using new values for K and ϵ as initial guesses

Results:

	$0.5 \cdot K_{a2}$	547 nm		562 nm		601 nm	
Guest G:	$2 \cdot K_{a1}$	ϵ_{HG}	ϵ_{HHG}	ϵ_{HG}	ϵ_{HHG}	ϵ_{HG}	ϵ_{HHG}
2	9498	862	0	2197	4627	1169	2356
<i>mPyPA</i>	8625	1446	0	4110	9608	2125	5270

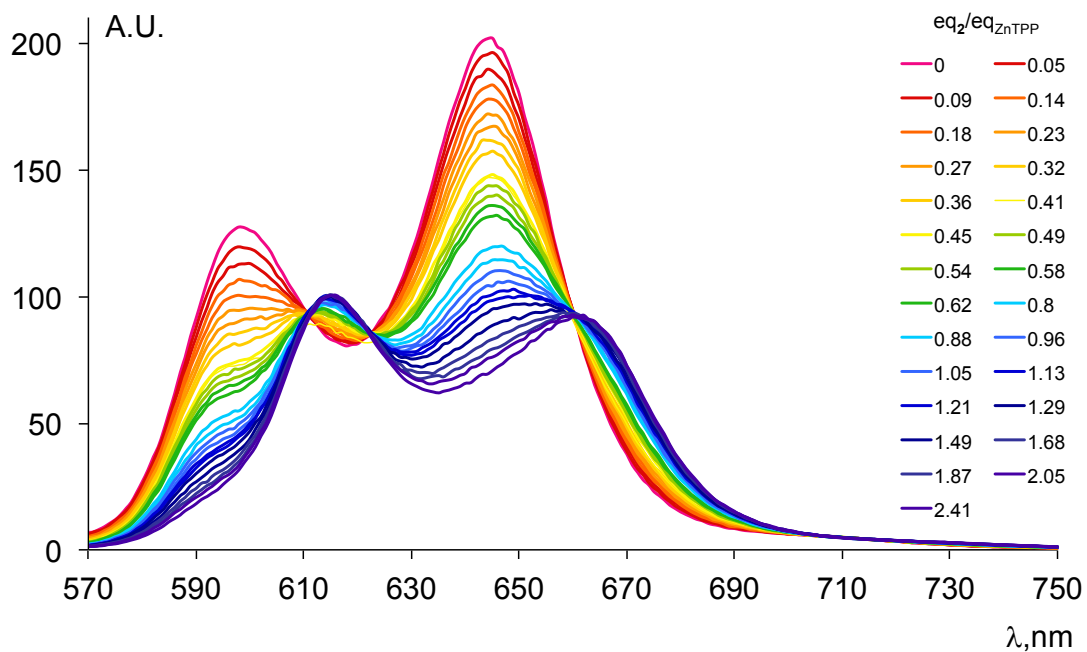


Figure S5 Luminescence spectra for the titration of ZnTPP with **2** in DCM. Excitation is at 555 nm, i.e., the isosbestic point seen during the UV-vis titration of the same solutions. The first point of the titration corresponds to pure ZnTPP ($8.8 \cdot 10^{-5}$ M, pink curve); the last point corresponds to a total addition of 2.4 equivalents of **2** (violet line).

NMR spectroscopy

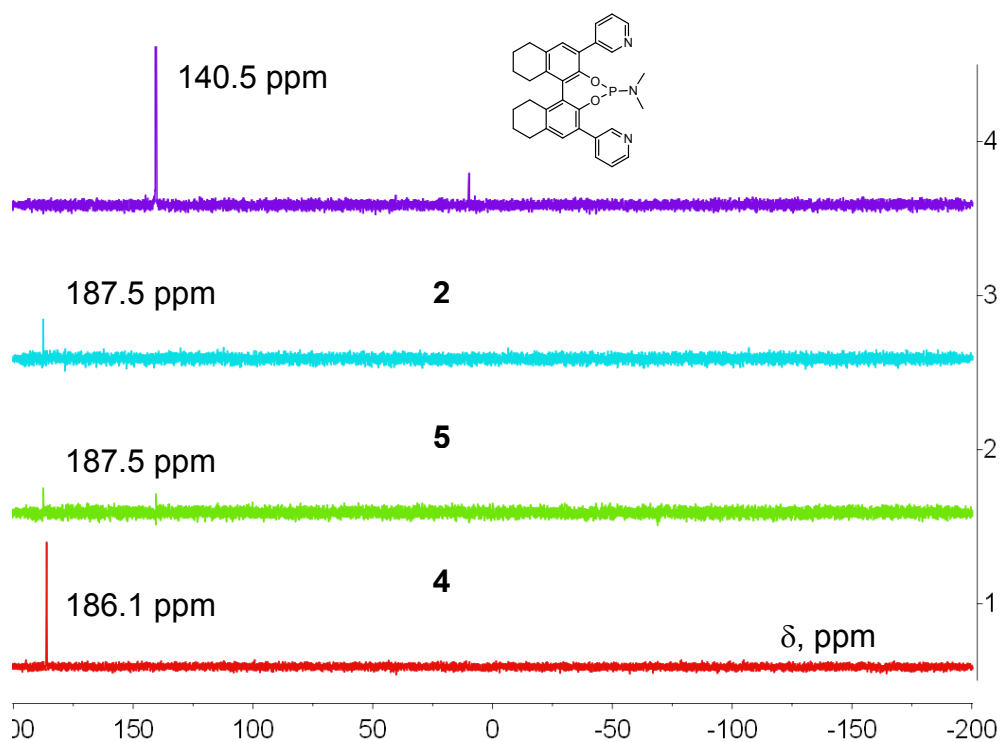


Figure S6 ^{31}P NMR spectra of the supramolecular ligand *m*PyPA and its complexes **2**, **4** and **5** in CDCl_3 .

Electrochemistry

Note: voltammograms for compounds **1** to **4** referenced to Ag/Ag⁺. A correction factor of -0.41V was used to convert to Fc/Fc⁺.

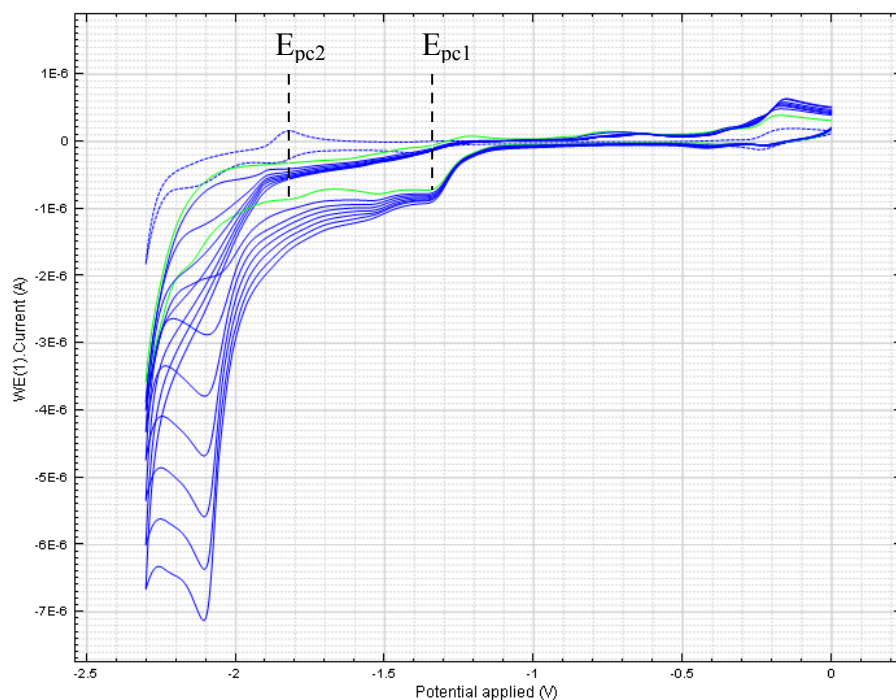


Figure S7 Cyclic voltammetry of **1** (1.0 mM) in butyronitrile containing 0.1 M *n*Bu₄NPF₆ with increasing acetic acid concentration: 0 (green), 1, 2, 3, 4, 5, 6, and 7 mM. Conditions: 293 K, static mercury drop working electrode, scan rate of 0.1 V s⁻¹.

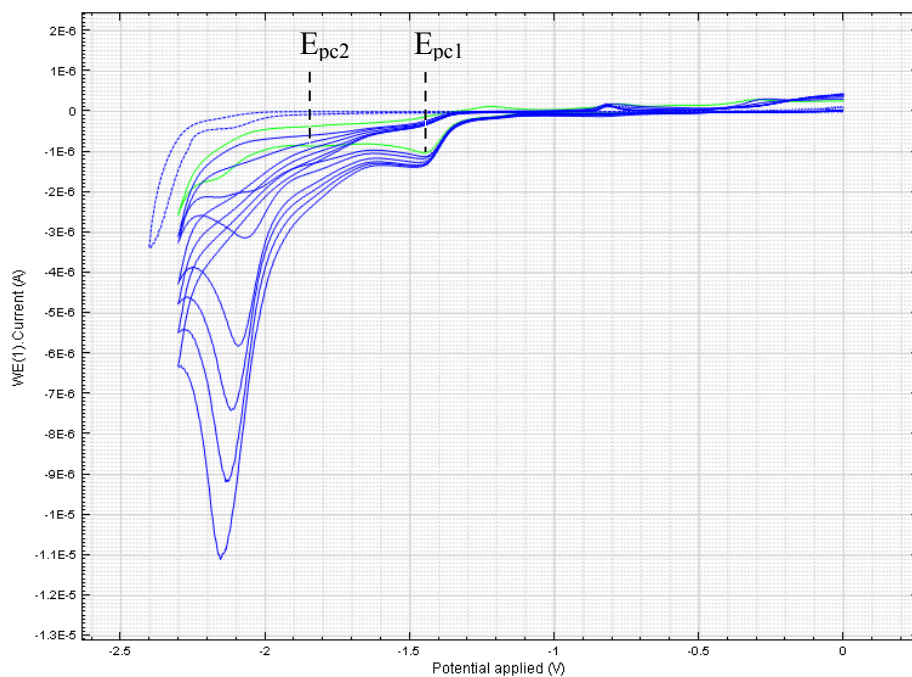


Figure S8 Cyclic voltammetry of **2** (1.0 mM) in butyronitrile containing 0.1 M *n*Bu₄NPF₆ with increasing acetic acid concentration: 0 (green), 1, 2, 4, 5, 6, and 7 mM. Conditions: 293 K, static mercury drop working electrode, scan rate of 0.1 V s⁻¹.

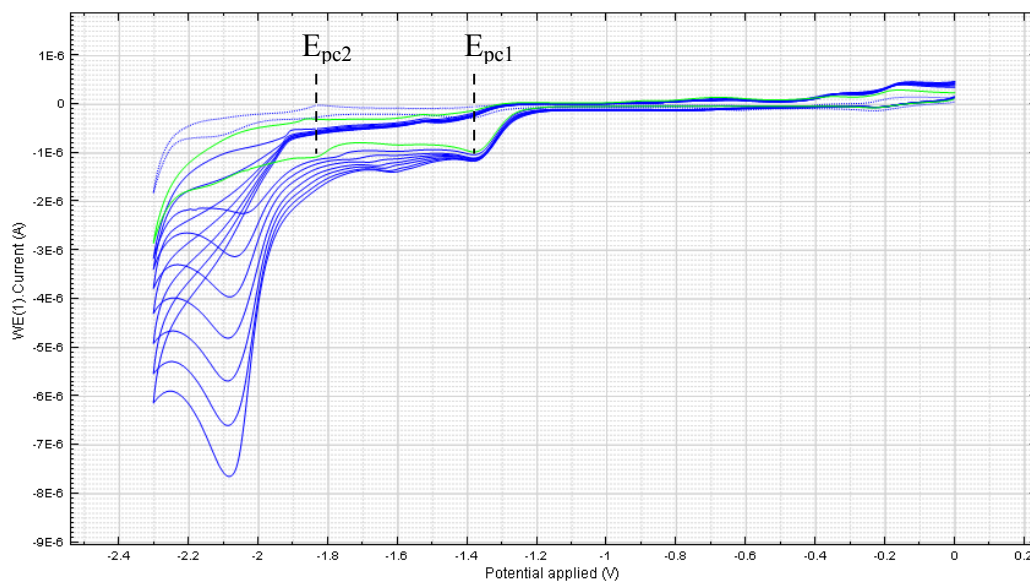


Figure S9 Cyclic voltammetry of **3** (1.0 mM) in butyronitrile containing 0.1 M $n\text{Bu}_4\text{NPF}_6$ with increasing acetic acid concentration: 0 (green), 1, 2, 3, 4, 5, 6, and 7 mM. Conditions: 293 K, static mercury drop working electrode, scan rate of 0.1 V s^{-1} .

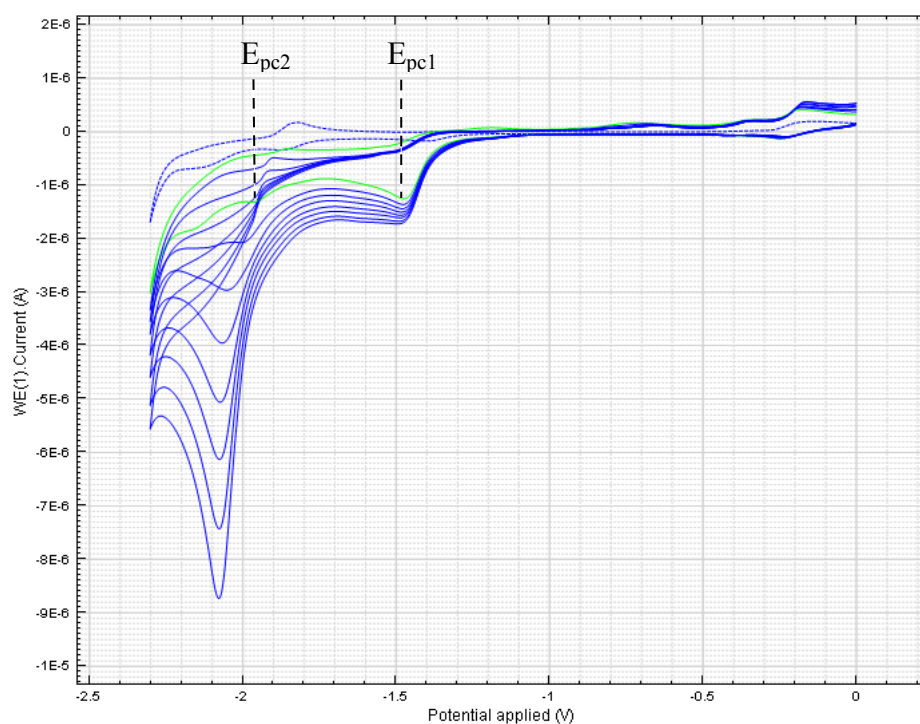


Figure S10 Cyclic voltammetry for **4** (1.0 mM) in butyronitrile containing 0.1 M $(n\text{Bu})_4\text{NPF}_6$ with increasing acetic acid concentration: 0 (green), 1, 2, 3, 4, 5, 6, and 7 mM. Conditions: 293 K, static mercury drop working electrode, scan rate 0.1 V s^{-1} .

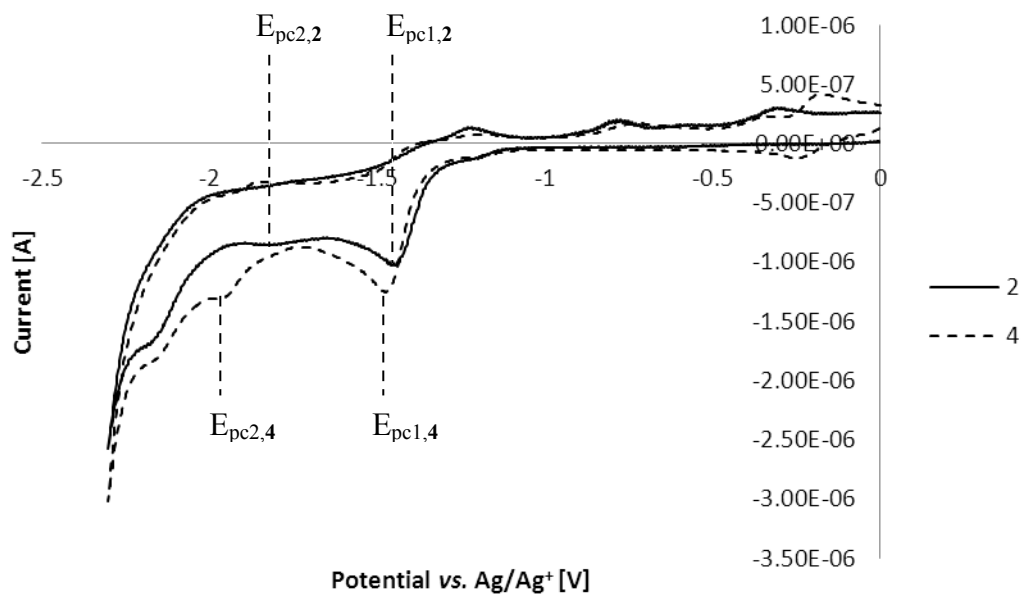


Figure S11 Comparison of cyclic voltammograms of **2** and **4** (1.0 mM) in butyronitrile containing 0.1 M $(n\text{Bu})_4\text{NPF}_6$. Conditions: static mercury drop working electrode, scan rate of 0.1 V s^{-1} .

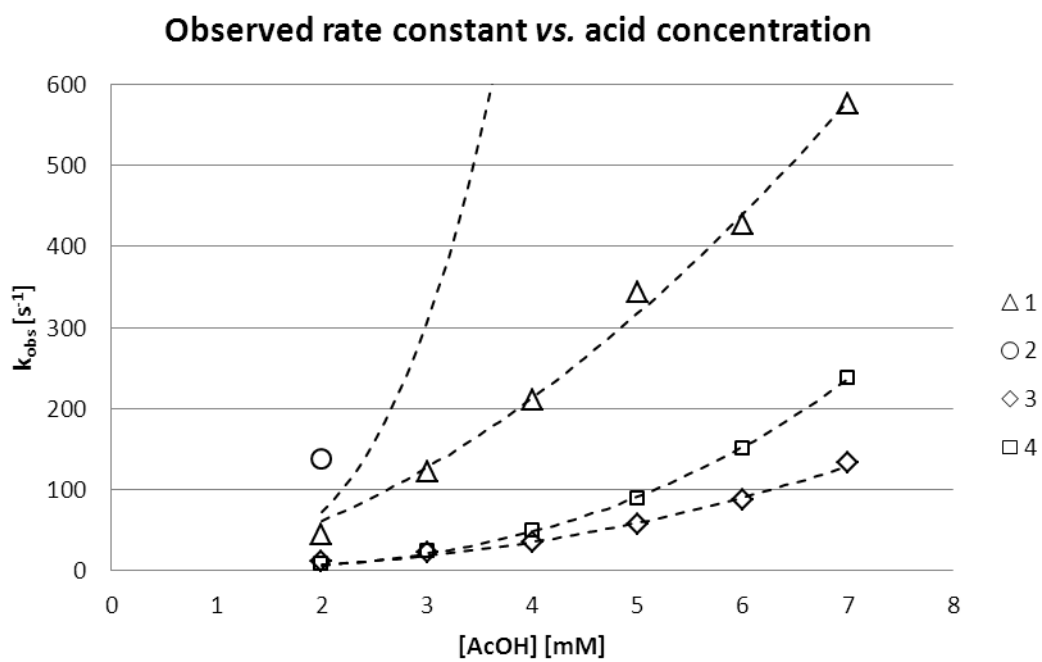


Figure S12 Observed rate constant vs. acetic acid concentration (detailed zoom from Fig. 4) with curve fits (dashed).

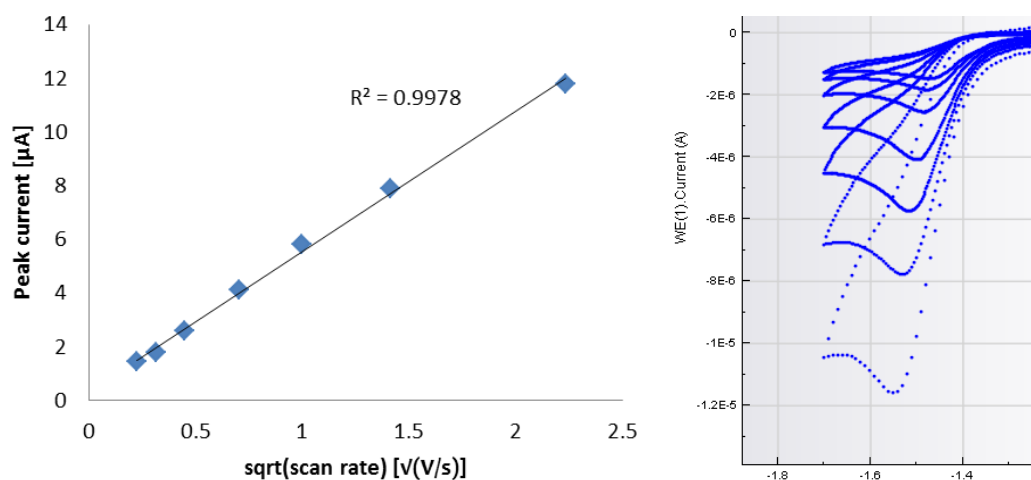


Figure S13 Peak current vs square root of scan rate for compound **2** (2.0 mM) in butyronitrile containing 0.1 M $(n\text{Bu})_4\text{NPF}_6$. Conditions: *static mercury drop* working electrode, scan rate of 0.05, 0.1, 0.2, 0.5, 1.0, 2.0 and 5.0 V s^{-1} .

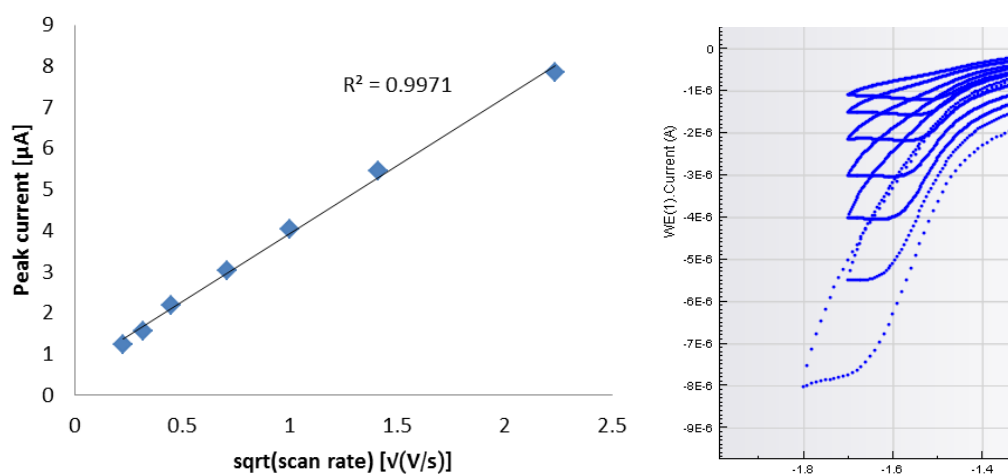


Figure S14 Peak current vs square root of scan rate for compound **2** (2.0 mM) in butyronitrile containing 0.1 M $(n\text{Bu})_4\text{NPF}_6$. Conditions: *platinum microdisc* working electrode, scan rate of 0.05, 0.1, 0.2, 0.5, 1.0, 2.0 and 5.0 V s^{-1} .

Table S1 Peak and catalytic currents and observed rate constants calculated by the

method of Dubois:
$$\frac{i_{cat}}{i_{pc2}} = \frac{n}{0.446} \cdot \sqrt{\frac{RT \cdot k_{obs}}{Fv}}$$

Compound	1		2		3		4	
i_{pc2} [μ A]	0.053		0.039		0.140		0.140	
eq. AcOH	i_{cat} [μ A]	k_{obs} [s^{-1}]	i_{cat} [μ A]	k_{obs} [s^{-1}]	i_{cat} [μ A]	k_{obs} [s^{-1}]	i_{cat} [μ A]	k_{obs} [s^{-1}]
2	0.80	44.2	1.04	138	1.07	11.3	0.95	8.9
3	1.33	122			1.50	22.3	1.56	24.1
4	1.75	212	2.78	986	1.90	35.7	2.24	49.7
5	2.23	343	3.78	1820	2.41	57.5	2.99	88.5
6	2.49	428	5.31	3600	2.96	86.7	3.91	151
7	2.89	577	7.05	6340	3.67	133	4.90	238

Table S2 Fitting parameters and quality (P = phosphine, PA = phosphoramidite)

	Ligand	Substituent	k'	n	Fit R^2
1	P	4-Pyridyl	17.8	1.79	0.9943
2	PA	3-Pyridyl	6	3.58	0.9988
3	P	Phenyl	1.44	2.31	0.9937
4	PA	Phenyl	0.934	2.845	0.9993

Infrared spectroscopy

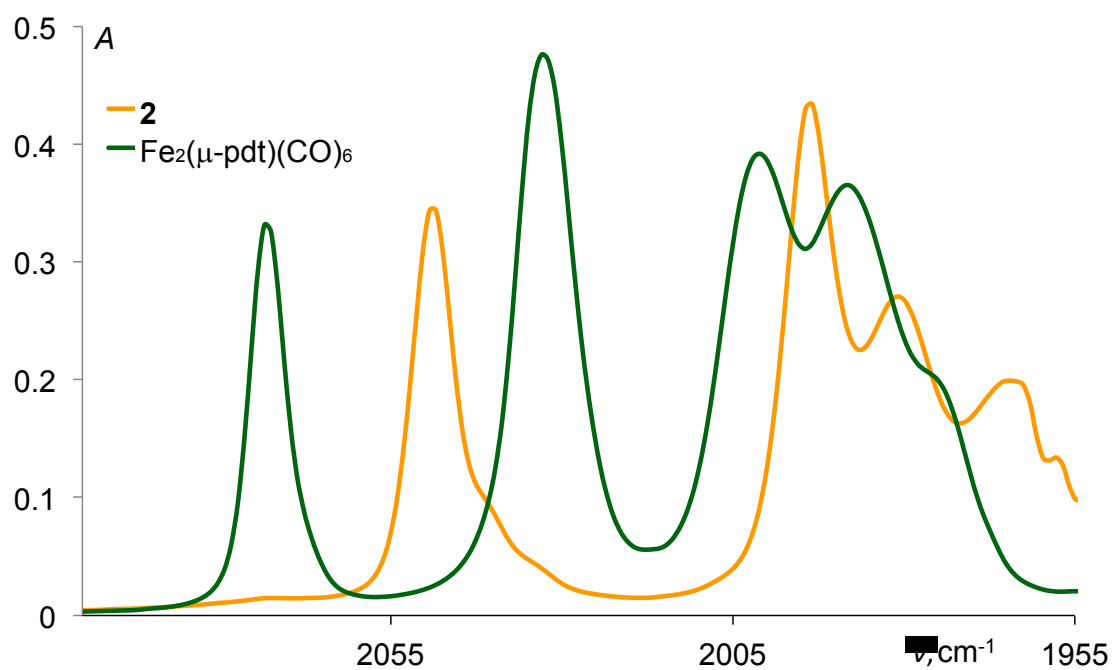


Figure S15 IR spectrum of the hexacarbonyl precursor, $[\text{Fe}_2(\mu\text{-pdt})(\text{CO})_6]$, and the monosubstituted complex **2** in toluene.

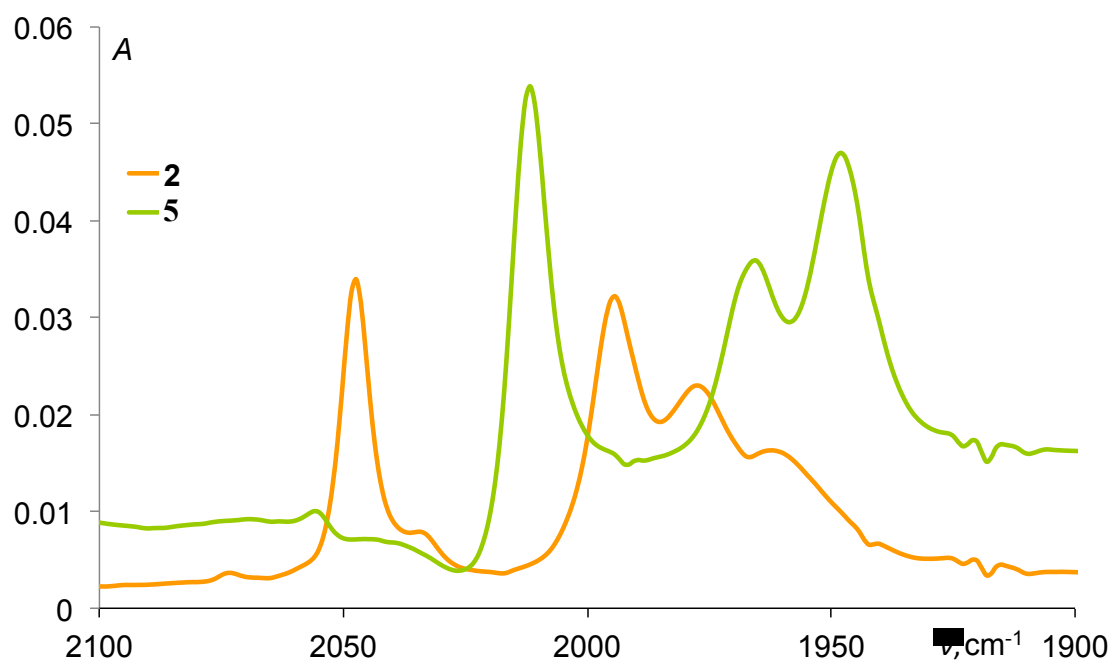


Figure S16 IR spectra of monosubstituted **2** and disubstituted **5** in dichloromethane.

Spectroelectrochemistry

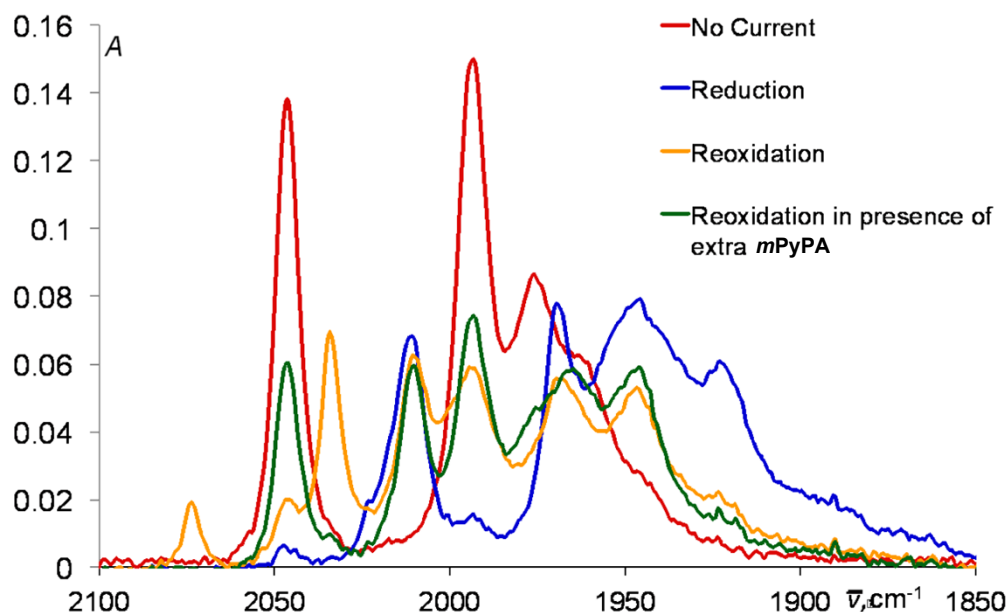


Figure S17 IR spectroelectrochemistry of **2** in butyronitrile: in absence of current (red); on the reduction wave (blue line) and after a single cycle of reduction and re-oxidation, in absence and presence of free phosphoramidite, *mPyPA* (yellow and green curves, respectively).

IR spectroelectrochemistry, carried out in the absence of a proton donor, indicates that **2** is not recovered after a cycle of reduction and re-oxidation; the deconvolution of the resulting spectrum reveals, instead, that the $[\text{Fe}_2(\mu\text{-pdt})(\text{CO})_6]$ complex and the disubstituted species, **5**, (binding two phosphoramidite ligands) were formed. This indicates that **2** disproportionates under electrochemical conditions at the cathode, in line with the behaviour of **1** observed during photocatalysis.⁵ However, when performing the spectroelectrochemistry measurement in presence of the free phosphoramidite ligand, compound **2** is regenerated after one cycle of reduction and re-oxidation, accompanied with some **5**; however, no sign of the $[\text{Fe}_2(\mu\text{-pdt})(\text{CO})_6]$ complex was observed. The IR spectrum recorded at the reduction wave (blue), shows some residual **2** (likely due to incomplete reduction) and mainly the disubstituted complex, **5**.

References

- 1) M. Krejčík, M. Daněk and F. Hartl, *J. Electroanal. Chem.*, 1991, **317**, 179.
- 2) M. Anouti, M. Caillon-Caravanier, C. Le Floch and Daniel Lemordant, *J. Phys. Chem. B*, 2008, **112**, 9406.
- 3) R. Bellini, S. H. Chikkali, G. Berthon-Gelloz and J. N. H. Reek, *Angew. Chem. Int. Edit.*, 2011, **50**, 7342.
- 4) C. F. Works, *J. Chem. Educ.*, 2007, **84**, 836.
- 5) P. Li, M. Wang, C. He, G. Li, X. Liu, C. Chen, B. Åkermark, and L. Sun, *Eur. J. Inorg. Chem.*, 2005, 2506.